AN ALTERNATE PROPOSAL FOR ARTM CPM

Erik Perrins
Department of Electrical and Computer Engineering
Brigham Young University
Provo, UT 84602
esp@ee.byu.edu

Faculty Advisor:
Michael Rice

ABSTRACT

Since the Advanced Range Telemetry (ARTM) program first proposed the use of multi-h continuous phase modulation (ARTM CPM), there has been much work done to characterize the performance of this waveform. The ideal performance of ARTM CPM is well understood and has been shown to be close to that of PCM/FM and the Tier I modulations (FQPSK-B and SOQPSK). In practice, however, ARTM CPM is very sensitive to phase noise at the receiver and also requires very long synchronization times. These difficulties can be addressed with additional link margin. In this paper we propose an alternate set of modulation indexes which are approximately 2 dB superior in performance with respect to the original set (we use minimum distance concepts to characterize the performance of each set). Brief consideration is also given to frequency pulses other than the existing raised cosine (RC) pulse. We also characterize the effect these new parameters have on the signal spectrum. This 2 dB gain gives ARTM CPM some of the system flexibility currently enjoyed by PCM/FM and the Tier I modulations. One such option is to realize this 2 dB gain using low-complexity *coherent* detection schemes, which we demonstrate; we also show a *noncoherent* detection scheme that performs within 2 dB of optimum (or in other words, it has the same performance as the existing *coherent* detector for ARTM CPM). This is significant since noncoherent detection avoids some of the synchronization burdens that have plagued ARTM CPM thus far.

INTRODUCTION

The ARTM Tier I and II modulation formats were chosen such that they have approximately the same detection efficiency as the legacy PCM/FM waveform, but with different degrees of spectral efficiency; however, the comparison of detection efficiency is somewhat unfair in that *suboptimum* detection schemes are used for PCM/FM and Tier I while the *optimum* detection scheme is used for ARTM CPM. In other

words, there is room for improvement in the case of PCM/FM and Tier I, while in all practicality ARTM CPM can only perform worse. In fact, Geoghegan has already shown for PCM/FM that a significant gain over limiter-discriminator detection is available through the use of multi-symbol noncoherent detection [1], while even more gain is possible using optimum coherent detection for PCM/FM. Thus, the level playing field for detection efficiency has already been broken up. The performance gap is widened further by the long synchronization times required by the fully coherent ARTM CPM detector and its sensitivity to phase noise [2].

In this paper, we present an alternate proposal for ARTM CPM which is approximately 2 dB superior to the existing ARTM CPM standard. We provide motivation for this proposal via minimum distance arguments which demonstrate that the existing set of modulation indexes for ARTM CPM, $h = \{4/16, 5/16\}$, are located at a relatively "weak" position in the performance space. This same analysis also shows a sharp increase in signal distance for the nearby set of proposed modulation indexes $h = \{5/16, 6/16\}$. We also briefly consider other frequency pulses of duration $L = 3$ symbol times, in addition to the existing 3RC pulse[1]. We show the effect these new parameters have on the signal spectrum.

This performance margin of 2 dB opens up the same possibilities that exist for PCM/FM and Tier I; in other words, we can pursue near-optimum detection techniques that realize as much of this gain as possible, or we can trade the gain for lower complexity (practical) detection schemes. For the sake of discussion, we divide complexity into the subcategories of *computational* complexity, in terms of the required number of trellis states and correlators (matched filters), and also into *system* complexity, including additional synchronization requirements, etc.

For both the existing and proposed configurations of ARTM CPM, a straightforward application of optimum detection principles [3] requires a detector with 128 matched filters followed by a maximum likelihood sequence estimator (MLSE) with 256 states. In terms of system complexity, this coherent detector requires carrier phase synchronization, symbol timing recovery, and modulation index synchronization. The mention of these synchronization requirements is important since their implementation is non-trivial; however, the details of their construction are beyond the scope of this paper. While coherent detection requires high *system* complexity, we show how it is possible to reduce the *computational* complexity with two different 32-state schemes that are within 0.1 dB of optimum. We also show a noncoherent detection scheme of 64 states that is within 2 dB of optimum, or approximately the same as the existing coherent detector for ARTM CPM. This noncoherent scheme avoids the system requirement of carrier phase recovery. We begin with a summary of the ARTM CPM signal model.

ARTM CPM SIGNAL MODEL

The existing parameters for the ARTM CPM are

$$M = 4, \qquad L = 3, \qquad h = \{4/16, 5/16\}$$
$$f(t) = \begin{cases} \frac{1}{2LT}\left[1 - \cos\left(\frac{2\pi t}{LT}\right)\right], & 0 \le t \le LT \\ 0, & \text{otherwise} \end{cases} \tag{1}$$

[1]We acknowledge that C. Bishop gave an informal presentation of some initial findings for different pulse shapes at ITC'03.

where the above parameters are explained in the following. The complex-baseband representation of the multi-h CPM signal, following standard notation [3], is given by

$$s(t,\boldsymbol{\alpha}) = \exp\big(j\psi(t,\boldsymbol{\alpha})\big), \tag{2}$$

$$\psi(t,\boldsymbol{\alpha}) = 2\pi \sum_{i=-\infty}^{n} \alpha_i h_{\underline{i}} q(t-iT), \qquad nT \le t < (n+1)T \tag{3}$$

where T is the symbol duration, $\{h_{\underline{i}}\}$ is the set of N_h modulation indexes ($N_h = 2$ in this case), $\boldsymbol{\alpha} = \{\alpha_i\}$ are the information symbols in the M-ary alphabet $\{\pm 1, \pm 3, \cdots, \pm(M-1)\}$, and $q(t)$ is the phase pulse. In this paper, the underlined subscript notation in (3) is defined as modulo-N_h, i.e. $\underline{i} \triangleq i \bmod N_h$. We assume the modulation indexes are rational numbers of the form [4]

$$h_{\underline{i}} = k_{\underline{i}}/p \tag{4}$$

where $k_{\underline{i}}$ and p are relatively prime integers. We note that many authors use the form $h_{\underline{i}} = 2k_{\underline{i}}/p$ for expressing the modulation indexes [3]. In a moment, we discuss the subtle difference between when these two expressions are used and the important advantage one obtains when using (4).

The phase pulse $q(t)$ and the frequency pulse $f(t)$ are related by

$$q(t) = \int_0^t f(\tau)\, d\tau. \tag{5}$$

The frequency pulse is supported over the time interval $(0, LT)$, as in (1), and is subject to the constraint

$$\int_0^{LT} f(\tau)\, d\tau = q(LT) = \frac{1}{2}. \tag{6}$$

Due to the finite duration of $f(t)$, the infinite sum in (3) can be divided into two terms

$$\psi(t,\boldsymbol{\alpha}) = \theta(t,\boldsymbol{\alpha}_n) + \pi \sum_{i=-\infty}^{n-L} \alpha_i h_{\underline{i}} \tag{7}$$

where

$$\theta(t,\boldsymbol{\alpha}_n) = 2\pi \sum_{i=n-L+1}^{n} \alpha_i h_{\underline{i}} q(t-iT). \tag{8}$$

The term $\theta(t,\boldsymbol{\alpha}_n)$ is a function of the *correlative state vector* $\boldsymbol{\alpha}_n = (\alpha_{n-L+1}, \alpha_{n-L+2}, \cdots, \alpha_n)$, which contains the L symbols being modulated by the phase pulse. There are M^L possible values for the correlative state vector. As it stands, the second term in (7) assumes one of $2p$ values when taken modulo-2π (this is because $\{h_{\underline{i}}\}$ are rational numbers). We consider the alternate data symbols $U_n = \big(\alpha_n + (M-1)\big)/2$ which are simply the result of a one-to-one mapping from values in the set $\{\pm 1, \pm 3, \cdots, \pm(M-1)\}$ to the values in the set $\{0, 1, \cdots, M-1\}$. Substituting $\alpha_n = 2U_n - (M-1)$ into (7) yields

$$\psi(t,\boldsymbol{\alpha}) = \theta(t,\boldsymbol{\alpha}_n) + \theta_{n-L} + \nu_n \tag{9}$$

where the *phase state* θ_{n-L} is given by

$$\theta_{n-L} = \frac{2\pi}{p}\left(\sum_{i=-\infty}^{n-L} U_i k_{\underline{i}}\right) \bmod p \tag{10}$$

and $\nu_n = \nu_{n-1} - \pi h_{\underline{n}}(M-1)$ is a data-independent phase tilt [4]. Due to (4), the phase state takes on only p distinct values $0, 2\pi/p, 2\cdot 2\pi/p, \ldots, (p-1)2\pi/p$. The structure of (9) is conveniently described by a phase trellis comprised of pM^{L-1} states, with M branches at each state. The optimum MLSE detector is based on this phase trellis. For ARTM CPM, this amounts to $pM^{L-1} = 256$ states, whereas this number would be 512 states without the use of the tilted phase model.

ALTERNATE PROPOSAL FOR ARTM CPM

We now develop a proposal for an alternate set of signal parameters given by

$$\begin{aligned} &M = 4, \qquad L = 3, \qquad h = \{5/16, 6/16\} \\ &f(t) = \begin{cases} \frac{1}{2LT}\left[1 - \cos\left(\frac{2\pi t}{LT}\right)\right], & 0 \le t \le LT \\ 0, & \text{otherwise} \end{cases} \end{aligned} \tag{11}$$

where the only difference from (1) is the set of modulation indexes $\{h_{\underline{i}}\}$. We begin with minimum distance analysis which is followed by analysis of the signal spectrum.

A. Minimum Distance Analysis

In [3, ch. 2], it is shown that the probability of bit error for CPM in additive white Gaussian noise (AWGN) is well approximated by

$$P_b \approx \sum_i C_i \cdot Q\left(\sqrt{d_i^2 \frac{E_b}{N_0}}\right) \tag{12}$$

where E_b is the signal energy per bit, N_0 is the one-sided power spectral density of the noise, C_i and d_i are constants that shall be explained shortly, and

$$Q(x) = \frac{1}{\sqrt{2\pi}} \int_x^\infty e^{-u^2/2}\, du. \tag{13}$$

Due to the nature of (13), as E_b/N_0 increases, the sum in (12) is dominated by the term with the smallest value of d_i. We refer to this value as $d_{\text{min}} = \min_i\{d_i\}$, or the *minimum normalized Euclidian distance*. This is significant because the error performance is conveniently summarized by this single distance parameter. The details required for computing d_{min} are found in [3, ch. 3].

A helpful design exercise is to fix the pulse shape and alphabet size (in this case the frequency pulse is 3RC and the alphabet size is $M = 4$) and compute d_{min} for a range of modulation indexes. Figure 1a shows d_{min}^2 for $M = 4$, 3RC, and for modulation indexes h_1 and h_2 that range from zero to one-half. There are four data points on this surface which are called out. The lower two points are for $(h_1, h_2) = (4/16, 5/16)$

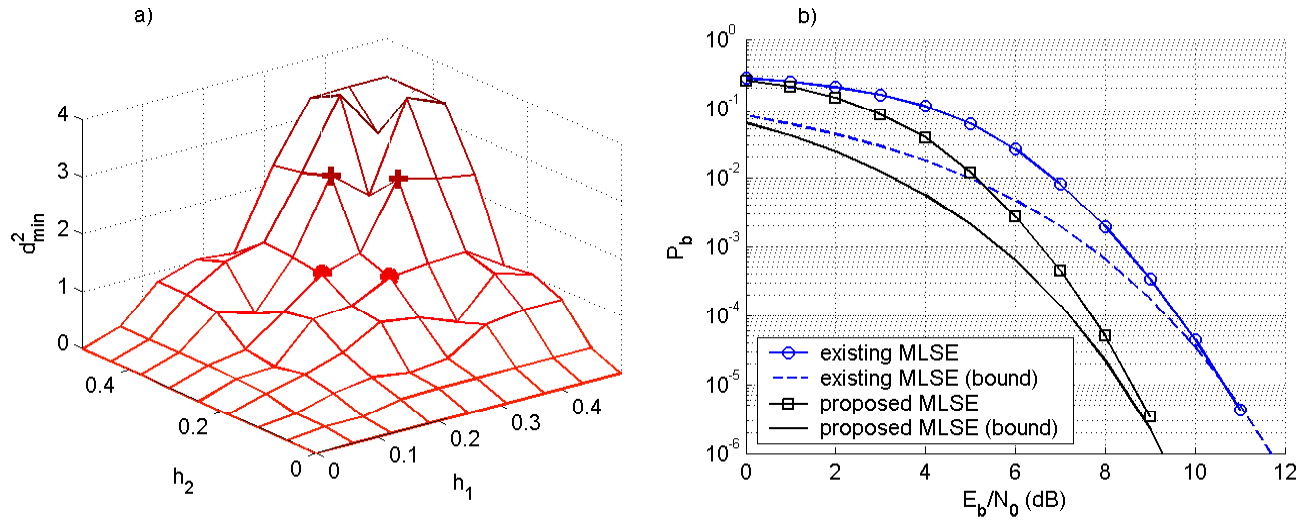

Figure 1: a) Minimum squared Euclidian distance over a range of modulation indexes. The '+' data points are for the proposed modulation indexes, the 'o' data points are for the existing modulation indexes. b) Performance curves for the existing and proposed schemes using Equation (12) and Table 1 (computer simulations are also shown). The curves show a performance advantage of slightly more than 2 dB for the proposed scheme at $P_b = 10^{-5}$.

Table 1: Parameters needed to compute Equation (12) for the existing and proposed ARTM CPM schemes.

Existing scheme

i	d_i^2	C_i
0	1.29	0.123
1	1.66	0.633

Proposed scheme

i	d_i^2	C_i
0	2.60	0.633
1	2.90	0.633

and $(h_1, h_2) = (5/16, 4/16)$, which is the existing ARTM CPM format, where $d^2_{\text{min}} = 1.29$. The upper two points are for $(h_1, h_2) = (5/16, 6/16)$ and $(h_1, h_2) = (6/16, 5/16)$, which is the proposed ARTM CPM format, where $d^2_{\text{min}} = 2.60$. The surface shows that the distance rises sharply in the region between these close values of modulation indexes and suggests a $10 \log_{10}(2.6/1.29) = 3$ dB gain is available simply by changing the modulation indexes.

As it turns out, both the existing and proposed ARTM CPM schemes have additional distance terms that make meaningful contributions to the sum in (12). Table 1 shows the important values of d_i^2 and C_i for each scheme; details regarding the derivation of these values are given in the Appendix. The values in Table 1 are used to generate the performance curves in Figure 1b, where corresponding curves from computer simulations are also displayed. For the existing scheme, the theoretical and simulated curves line up exactly for large E_b/N_0, which confirms the completeness of the listing in Table 1. For the proposed scheme, there are numerous less-significant terms which are not given in Table 1 that account for the slight difference between the theoretical and simulated curves. The curves in Figure 1b give the best view of the performance advantage of the proposed scheme, which is slightly larger than 2 dB at $P_b = 10^{-5}$.

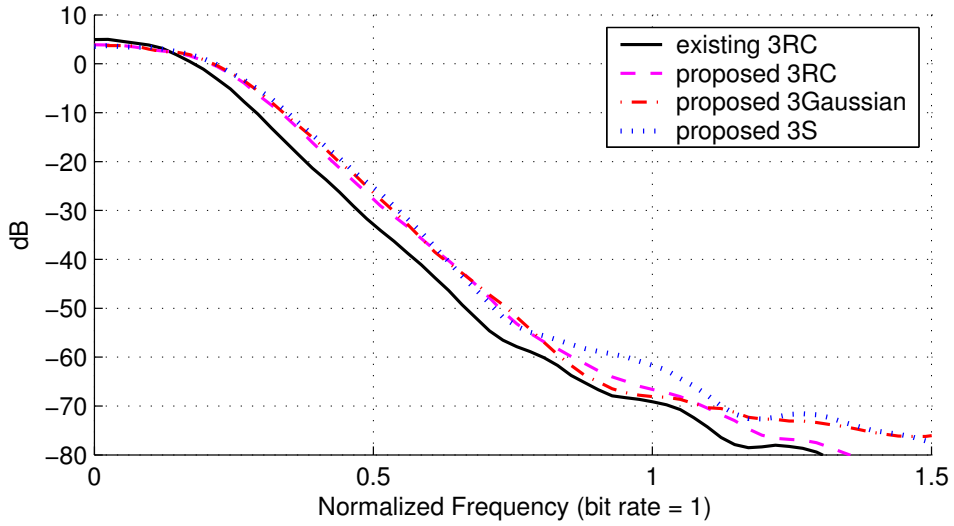

Figure 2: PSD of the proposed modulation indexes using three different pulse shapes (3RC, 3Gaussian, and 3S), these are compared to the PSD of the existing 3RC scheme.

B. Spectral Analysis

Figure 2 shows the power spectral density (PSD) of the existing 3RC scheme. Also shown in the figure are three PSDs for the proposed modulation indexes using different length-$3T$ frequency pulse shapes: RC, Gaussian [3, ch. 2], and the so-called *S* pulse[2] These pulses lead to slightly different spectral *and* distance characteristics; as an informal rule, the 3Gaussian pulse results in an additional gain of 0.25 dB for all of the proposed detection schemes that follow, while the 3S pulse results in a gain of 0.35 dB. With this rule in mind, the remainder of the discussion is in terms of the 3RC pulse.

REDUCED COMPLEXITY DETECTION SCHEMES

As mentioned earlier, the optimal coherent detector for ARTM CPM requires $pM^{L-1} = 256$ states and 128 correlators (matched filters). The impulse response of each filter has a duration of one symbol time. This detector is described in detail in [3, ch. 7]. Since the proposed ARTM CPM scheme leaves the values of M, L, and p unchanged, the number of states and matched filters remain unchanged as well; in terms of computational complexity, the two schemes belong to the same complexity "family". We have already seen the performance of these two optimal detectors in Figure 1b.

For coherent detection, there are a number of complexity reduction schemes available. From a performance standpoint, the two most attractive of these are the pulse amplitude modulation (PAM) technique [5], and the one given by Svensson, Sundberg, and Aulin (SSA) [6]. The details needed to describe these detectors are too numerous to be given here; however, these detection schemes are surveyed in [7] for the existing ARTM CPM waveform. In short, these two approximations can be paired with yet an-

[2]The S pulse of length-$3T$ is simply a length-T rectangular pulse convolved with itself twice.

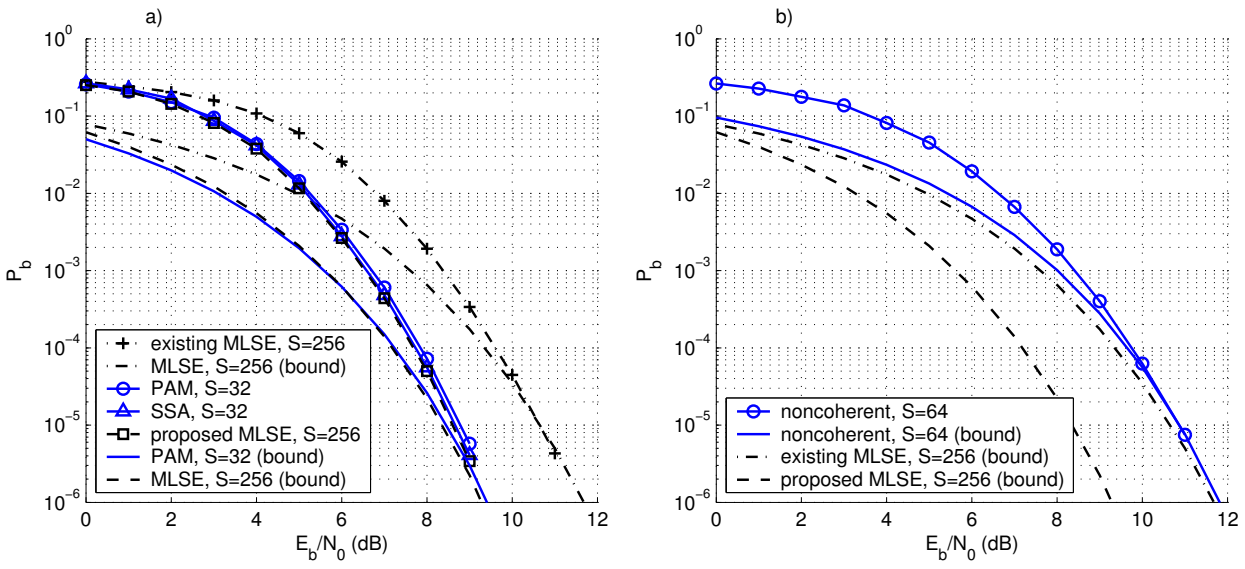

Figure 3: a) Performance of the PAM and SSA reduced-complexity coherent detectors for the proposed ARTM CPM scheme (both of these detectors have $S = 32$ states). For reference, the optimum performance curves for both modulation schemes are also shown, as well as a performance bound for the PAM detector. The SSA detector has essentially optimum performance while the PAM detector is within a tenth of a dB of optimum. b) Performance of the noncoherent detector from [9]. A noncoherent configuration with $S = 64$ states for the proposed ARTM CPM scheme has roughly the same performance as the coherent detector for the existing scheme. This is confirmed with a performance bound and computer simulations (both shown).

other approximation (reduced state sequence estimation, or RSSE [8]) to each yield a 32-state detector. While these two detectors use the same trellis, they have an entirely different matched filter bank. The SSA detector requires 32 matched filters where the PAM detector requires the equivalent of 24 matched filters[3]. Figure 3a shows the simulated performance of these two 32-state detectors; this figure also shows the reference curves from Figure 1b, as well as a theoretical bound for the PAM detector. The 32-state SSA detector has essentially the same performance as the optimum 256-state detector, while the 32-state PAM detector is within a tenth of a dB of optimum.

Turning our attention to noncoherent detection, there are also a number of schemes available for ARTM CPM [7]. Of these, the one in [9] shows the most promise, both in terms of performance and low computational complexity. Based on the distance analysis in [10], this *noncoherent* detector in a 64-state configuration has an equivalent squared Euclidian distance of 1.46 for the proposed scheme; this value is comparable to the *coherent* distance properties of the existing ARTM CPM scheme, shown in Table 1. Figure 3b shows the reference curves from Figure 1b along with the noncoherent performance bound, which is verified with computer simulations (also shown).

[3]For the proposed scheme, the PAM detector actually uses just four matched filters; these filters are longer than the SSA filters and are thus the computational equivalent of 24 SSA-type filters. For the existing ARTM CPM scheme, the PAM detector performs well with only three matched filters, which are the computational equivalent of 18 SSA-type filters [7].

CONCLUSION

We have proposed an alternate set of modulation indexes for ARTM CPM. In doing so, we have shown how these proposed parameters achieve a 2 dB performance gain over the existing ARTM CPM scheme with a modest increase in signal spectrum. Assuming these spectral properties are satisfactory, we have also shown a number of detection schemes that present different options for this 2 dB gain; the reduced-complexity coherent detectors allow an attractive means of realizing this gain, while the noncoherent detector trades this gain for reduced system complexity and achieves performance comparable to the existing ARTM CPM scheme. We have also shown that minor gain increments are available from the use of frequency pulses other than the existing raised cosine pulse. This proposal gives the ARTM CPM modulation some of the system flexibility enjoyed by the ARTM Tier I modulations and the legacy PCM/FM waveform.

APPENDIX

We show how to arrive at the values given in Table 1. For CPM, the bit error probability is approximately [3, ch. 2]

$$P_b \approx \sum_i C_i \cdot Q\left(\sqrt{d_i^2 \frac{E_b}{N_0}}\right). \tag{14}$$

The normalized squared Euclidian distance d_i^2 is [3, ch. 2]

$$\begin{aligned} d_i^2 &= \frac{\log_2 M}{2} \int \left| s(t, \boldsymbol{\alpha}_j) - s(t, \boldsymbol{\alpha}_k) \right|^2 dt & (15) \\ &= \log_2 M \int \left[1 - \mathrm{Re}\{ s(t, \boldsymbol{\gamma}_i) \} \right] dt & (16) \end{aligned}$$

where $\boldsymbol{\gamma}_i = \boldsymbol{\alpha}_j - \boldsymbol{\alpha}_k$ is the *difference* between two data sequences $\boldsymbol{\alpha}_j$ and $\boldsymbol{\alpha}_k$. The integral in (16) will continue to grow indefinitely except for a special class of $\boldsymbol{\gamma}_i$, called *signal merges*, which satisfy the condition

$$\left(\sum_l \gamma_l k_{\underline{l}} \right) \bmod 2p = 0 \tag{17}$$

where $k_{\underline{l}}$ and p are from the modulation indexes in (4). In words, a merge is when the phase advances and retards over a brief time interval such that the net change in phase is zero, when taken modulo 2π. For example, with the existing ARTM CPM modulation indexes, if we insert the example difference sequence $\boldsymbol{\gamma}_{\text{ex}} = \cdots, 0, 0, 2, -4, 6, -4, 2, 0, 0, \cdots$ into (17) we get $\cdots 0 + 2 \cdot 4 - 4 \cdot 5 + 6 \cdot 4 - 4 \cdot 5 + 2 \cdot 4 + 0 + \cdots = 0$. This example sequence is a signal merge since its coordinates sum to zero when scaled by the modulation indexes. We point out that for multi-h CPM, a merge also depends on the alignment of the modulation indexes with the difference sequence. In this example, we designate $h_0 = 4/16$ as the modulation index that coincides with the first non-zero coordinate, 2, of $\boldsymbol{\gamma}_{\text{ex}}$.

Of course, there is more than one $(\boldsymbol{\alpha}_j, \boldsymbol{\alpha}_k)$ pair that has the common difference $\pm\boldsymbol{\gamma}_i$. We must count

Table 2: Merge parameters for the existing case with $M = 4$, 3RC, and $h = \{4/16, 5/16\}$.

i	$\boldsymbol{\gamma}_i$	d_i^2	C_i	R	h_0	$W(\boldsymbol{\gamma}_i)$	$N(\boldsymbol{\gamma}_i)$
0	$\cdots, 0, 2, -4, 6, -4, 2, 0, \cdots$	1.29	0.123	5	$4/16$	7	72
1	$\cdots, 0, 2, -2, 0, 2, -2, 0, \cdots$	1.66	0.633	5	$4/16$	4	648

Table 3: Merge parameters for the proposed case with $M = 4$, 3RC, and $h = \{5/16, 6/16\}$.

i	$\boldsymbol{\gamma}_i$	d_i^2	C_i	R	h_0	$W(\boldsymbol{\gamma}_i)$	$N(\boldsymbol{\gamma}_i)$
0	$\cdots, 0, 2, -2, 0, 2, -2, 0, \cdots$	2.60	0.633	5	$5/16$	4	648
1	$\cdots, 0, 2, -2, 0, 0, 0, 2, -2, 0, \cdots$	2.90	0.633	7	$5/16$	4	10368

these pairs, which is simply the number

$$N(\boldsymbol{\gamma}) = 2 \prod_{l=0}^{R-1} \left(M - \frac{|\gamma_l|}{2} \right) \tag{18}$$

where R is the span of non-zero coordinates in $\boldsymbol{\gamma}$. Using $\boldsymbol{\gamma}_{\text{ex}}$ again, we have $R = 5$ and $N(\boldsymbol{\gamma}_{\text{ex}}) = 2 \cdot 3 \cdot 2 \cdot 1 \cdot 2 \cdot 3 = 72$, meaning there are 72 pairs of data sequences with the common difference of $\pm\boldsymbol{\gamma}_i$.

These difference sequences are *error events*. In order to arrive at a bit error probability, we must count the number of bit errors in an error event. This number is a function of the mapping from bits to symbols, which is typically a Gray code. In our example, the bit error weight is $W(\boldsymbol{\gamma}_{\text{ex}}) = 7$ bits.

With these quantities defined, the scale factor C_i is given by [10]

$$C_i = \frac{W(\boldsymbol{\gamma}_i) \cdot N(\boldsymbol{\gamma}_i)}{\log_2 M \cdot N_h \cdot M^R}. \tag{19}$$

In Tables 2 and 3 we show the intermediate quantities needed to compute (19) for the existing and proposed ARTM CPM schemes respectively.

REFERENCES

[1] M. Geoghegan. "Improving the detection efficency of conventional PCM/FM telemetry by using a multi-symbol demodulator". In *Proceedings of the International Telemetering Conference*, San Diego, CA, October 2000.

[2] K. Temple. "ARTM Tier II waveform performance". In *Proceedings of the International Telemetering Conference*, Las Vegas, NV, October 2003.

[3] J. B. Anderson, T. Aulin, C-E. Sundberg. *Digital Phase Modulation*. Plenum Press, New York, 1986.

[4] B. E. Rimoldi. "A decomposition approach to CPM". *IEEE Trans. Inform. Theory*, 34:260–270, March 1988.

[5] E. Perrins and M. Rice. "Optimal and reduced complexity receivers for M-ary multi-h CPM". In *Proceedings of the IEEE Wireless Communications and Networking Conference, WCNC'04*, Atlanta, Georgia, March 2004.

[6] A. Svensson, C-E. Sundberg, and T. Aulin. "A class of reduced-complexity viterbi detectors for partial response continuous phase modulation". *IEEE Trans. Commun.*, 32:1079–1087, Oct. 1984.

[7] E. Perrins and M. Rice. "Survey of detection methods for ARTM CPM". In *Proceedings of the International Telemetering Conference*, San Diego, CA, October 2004.

[8] A. Svensson. "Reduced state sequence detection of partial responce continuous phase modulation". *IEE Proc., pt. I*, 138:256–268, Aug. 1991.

[9] E. Perrins and M. Rice. "Multi-symbol noncoherent detection of multi-h CPM". In *Proceedings of the International Telemetering Conference*, Las Vegas, NV, October 2003.

[10] E. Perrins and M. Rice. "On noncoherent detection of CPM". *submitted for publication in IEEE Journal on Selected Areas in Communications (please contact authors for a copy)*.